

Effect of fluorine on the structural and electronic properties of *a*-Si:H:F

A. A. Langford, A. H. Mahan, M. L. Fleet, and J. Bender

Solar Energy Research Institute, 1617 Cole Boulevard, Golden, Colorado 80401

(Received 21 December 1988; revised manuscript received 6 November 1989)

The effects of fluorine incorporation on the microstructural and electronic properties of *a*-Si:H:F with 1–7 at. % F have been systematically studied. Infrared spectra show that as the fluorine content increases, silicon dihydride bonding increases. Density measurements confirm that this is associated with an increase in microvoid content, suggesting that fluorine induces the formation of voids which are lined with SiH₂. With the increase in F and SiH₂, the photoconductivity of the material decreases over 4 orders of magnitude. A review of the literature shows that the appearance of SiH₂ is a universal result of > 1 at. % F incorporation by many techniques and is not limited to the present study. Mechanisms by which fluorine can induce structural changes are evaluated. These results are contrasted with the use of fluorinated process gases to deposit microcrystalline films and Si-Ge alloys. This has implications for the incorporation of fluorine in photovoltaic devices.

I. INTRODUCTION

The suggestion by Madan *et al.*¹ of improved electronic properties from the incorporation of fluorine in amorphous silicon spurred extensive research into the preparation of *a*-Si:H:F. In the initial work, films fabricated by a glow discharge of SiF₄ and H₂ were reported to have a low density of localized states (particularly near the surface²), no photoinduced degradation, and high conductivity when doped. The subsequent scientific literature seems to be divided between reports of enhancement and reports of degradation of the film properties with F incorporation. In reviewing the literature, we need to differentiate between fluorinated amorphous silicon and amorphous silicon deposited using fluorinated process gases but which contains < 1 at. % F. In particular, we confine comparisons in the following discussion to films containing typically 1–5 at. % F, although this range may extend to 15 at. % F in some reports.

In agreement with Madan's results, other researchers reported^{3,4} device quality *a*-Si:H:F fabricated in a glow discharge of SiF₄ and SiH₄, or SiH₂F₂. In contrast, several other groups report a lower photoconductivity in *a*-Si:H:F (Refs. 5–8) and *a*-Si:F.^{9,10} Usui *et al.*⁵ specifically show a decrease in the dark and photoconductivity as the mole fraction of SiF₄ increases in a glow discharge of SiH₄ in Ar. Similarly, Carlson and Smith⁶ found that the conversion efficiency of *p-i-n* solar cells decreases as SiF₄, HF, or F₂ is added to a SiH₄ discharge during the *i*-layer deposition.

A potential advantage of fluorine over hydrogen is the higher strength of the Si—F bond. This may be expected to improve the termination of Si dangling bonds and provide increased thermal stability and decreased photodegradation. Again, experimental results vary in their support of this proposition. It has been demonstrated using *a*-Si:F that fluorine is able to passivate dangling bonds¹¹ but the spin density is still as high^{11,12} as in *a*-Si:H or higher.¹³ Several groups report that the light-induced de-

gradation of the dark conductivity^{1,3,7} or photoconductivity¹² is less severe in fluorinated films, although this comparison is limited when the films are not initially of device quality. It was also reported⁹ that fluorination made *a*-Si:F more heat resistant since the F content, infrared spectra, and temperature dependence of the dark conductivity were unchanged after annealing to 600 °C. However, another annealing study¹¹ shows that SiF₄ bubbles form inside *a*-Si:F with heating to 450 °C.

Because fluorine attacks Si—Si bonds, it was proposed that it would etch the surface during growth and improve the film microstructure.¹⁴ However, based on thermodynamic considerations the opposite has also been argued.¹⁰ Since the formation of any Si—F bond reduces the system free energy, fluorine can bond at any site it encounters in the network. This is contrasted with hydrogen which, because of the lower strength of the Si—H bond, migrates on the surface and preferentially dissociates strained Si—Si bonds. Support for the latter view comes from Raman spectra¹⁵ which show that *a*-Si:F has a wider bond angle distribution than *a*-Si:H, which generally indicates a greater lattice strain. On the other hand, the Raman spectra could also be interpreted as evidence that the greater ionicity of the Si—F bond compared to Si—H imposes less bond angle constraint.¹⁴

To investigate the effect of fluorine on amorphous silicon, we deposited a series of films with 1–7 at. % fluorine. We report here on systematic changes in structural and electrical properties with fluorine incorporation. Mechanisms by which fluorination could affect the lattice structure are discussed. The results are compared with other published work, particularly with reports that the use of fluorinated process gases leads to enhanced microcrystallization of *a*-Si:H(F) and microstructural changes in *a*-Si-Ge:H(F) alloys.

II. EXPERIMENT

Films of *a*-Si:H:F were deposited by direct photochemical vapor deposition (photo-CVD) of Si₂H₆ with a low-

pressure Hg lamp. The fluorine source is XeF₂, which reacts with Si₂H₆ to form partially fluorinated disilanes. XeF₂ is an etchant for silicon which was initially introduced to solve the problem of window clouding in photo-CVD.¹⁶⁻¹⁸ XeF₂ in He carrier gas is directed at the window to continuously etch it clean. The disilane is introduced upstream of the photolysis region and a film deposits on the heated substrate placed parallel to the window. Details of the deposition technique are described elsewhere.¹⁶

Six series of films were deposited: two in which the XeF₂ flow was varied at fixed substrate temperatures, $T_S = 245$ and 270 °C, one with fixed flows rates and varying substrate temperature, two in which dilution in H₂ was varied with fixed XeF₂ and Si₂H₆ flows, and one with varying partial pressure of Si₂H₆. The deposition parameters are listed in Table I. In the H₂ dilution experiments, the total pressure and total flow rates were kept constant while H₂ was partially substituted for He as a diluent gas. Similarly, in the Si₂H₆ partial pressure experiments, $P_{\text{Si}_2\text{H}_6}$ was increased while decreasing P_{He} but maintaining constant total flow and pressure. Films were simultaneously deposited on single-polished *c*-Si and on Corning 7059 glass substrates.

Typical impurity levels in the films determined by secondary-ion mass spectrometry (SIMS) are $(1-2) \times 10^{19}$ cm⁻³ carbon, $(1-2) \times 10^{18}$ cm⁻³ nitrogen, and $(5-20) \times 10^{19}$ cm⁻³ oxygen. The films on *c*-Si substrates were analyzed for fluorine content by x-ray photoelectron spectroscopy (XPS) and electron probe microanalysis (EPMA), and for bonded fluorine and hydrogen content by ir spectroscopy. Films on Corning 7059 glass substrates were used for electrical and optical measurements. The coplanar conductivity was measured using a General Electric ELH projection lamp with a white light flux of 100 mW/cm². The spectral distribution of the lamp was measured and used along with the reflectance, transmittance, and photoconductivity of each film to obtain $\eta\mu\tau$, the product of the carrier generation efficiency, electron mobility, and lifetime. The activation energy was obtained from measurements of the dark conductivity over the temperature range of 60–180 °C. The optical gap was determined from a Tauc plot¹⁹ of the visible transmission

spectrum. Raman spectra were measured in the almost backscattering geometry using 50 mW of the 514.5-nm Ar⁺ laser line. The thickness was measured with a Tencor alpha-step profiler. The films were limited to a typical thickness of 3000 Å by the deposition rate of <0.5 Å/s.

The primary tool for examining the hydrogen and fluorine in the films was infrared spectroscopy. Spectra were measured with either a Nicolet 7199 FTIR at 2-cm⁻¹ resolution or a Perkin-Elmer 580B at 6.8-cm⁻¹ resolution. No significant difference was found in the results from the two spectrometers. The absorbances of the silicon hydride and fluoride bands were integrated using the method described by Brodsky²⁰ with substrate transmittance $T_0 = 0.54$.²¹ In cases of two overlapping peaks, they were deconvoluted assuming Gaussian line shape. The sources of uncertainty in the integrated absorbances, on the order of 20%, come from peak deconvolution, locating the baseline when peaks overlap, and film-thickness nonuniformity. The hydrogen content was calculated from the integrated absorbance of the 630-cm⁻¹ peak.²²

III. RESULTS

A. Effect of *F* on structure

1. Infrared spectra

Infrared spectra are an excellent indicator of the fluorine bonding configuration. Figure 1 shows the Si—F stretching region of a spectrum and Fig. 2 shows a set of typical spectra of films with varying fluorine content. The fluorine absorption bands identified in the literature^{23,24} are the Si—F stretch at 830 cm⁻¹, the SiF₂ stretch at 930 cm⁻¹, and the SiF₄ stretch at 1015 cm⁻¹. The shoulder at 980 cm⁻¹ is not definitively assigned but we previously observed it¹⁶ and suggested it could be due to SiF₃ or, more probably, (SiF₂)_{*n*}. These assignments are summarized in Table II. At constant deposition temperature as the total F content is increased, the absorbances of the various SiF_{*n*} species increase in constant proportion to one another (Fig. 3).

We calibrated the sum of the integrated ir absorbances of the Si—F stretch bands to the F content measured by

TABLE I. Deposition parameters. One parameter was varied in each series.^a

Series symbol	Varied parameter	Flow (sccm)		Partial pressure (Torr) ^b			<i>T</i> (°C)
		XeF ₂	Si ₂ H ₆	He	H ₂		
○	flow (XeF ₂)	0.03–0.95 ^c	2.3	0.7	0	245	
□	flow (XeF ₂)	0.03–0.48	2.3	0.7	0	270	
+	<i>T</i> _{substrate}	0.09	2.3	0.7	0	245–350	
×	<i>P</i> _{Si₂H₆}	0.03	0.3–2.3	2.7–0.7	0	245	
▲	H ₂ dilution	0.06	0.3	0.3–2.7	2.4–0	245	
△	H ₂ dilution	0.12	0.3	0.3–2.7	2.4–0	245	

^aSome samples fit into two of the series of parameter variations and so two symbols are superimposed in the following figures.

^bThe total pressure is 3 Torr for all depositions.

^cThese correspond to partial pressures of 1.5–45 mTorr.

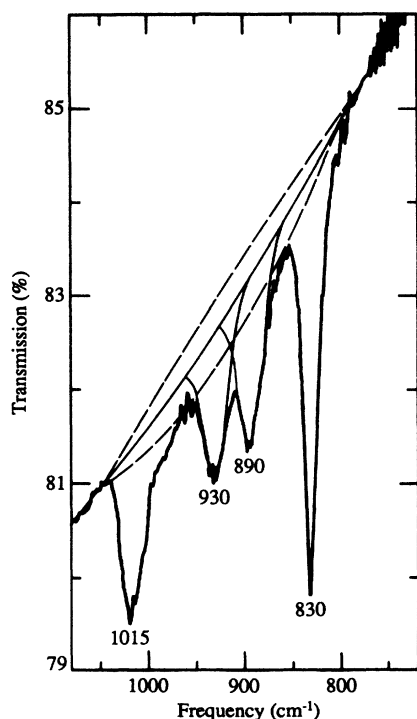


FIG. 1. Si—F stretch region of ir spectrum of *a*-Si:H:F deposited at substrate temperature 245 °C, with 5.8 at. % F and thickness 3900 Å. The upper and lower baselines were used to estimate the uncertainty in the integrated absorbance. The SiH₂ bend at 890 cm⁻¹ is deconvoluted from the SiF₂ stretch at 930 cm⁻¹ using Gaussian line shapes.

XPS and EPMA, and found that they are linearly related with the proportionality $11 \pm 1 \text{ cm}^{-1}/\text{at. \% F}$.²⁵ The fluorine content ranges from 0.5% with $T_S = 350^\circ\text{C}$ and XeF₂ flow 0.09 sccm (cubic centimeters at STP) to 7.5% with $T_S = 245^\circ\text{C}$ and XeF₂ flow 0.95 sccm. In this report, we use Si—F to refer to silicon-fluorine bonds in all species and SiF to identify silicon monofluoride specifically.

The modes associated with hydrogen are the SiH stretch at 2000 cm⁻¹, the SiH₂ stretch at 2080 cm⁻¹, the SiH₂ bend at 890 cm⁻¹, and both the SiH bend and SiH₂

TABLE II. Assignments of infrared peaks.

Frequency (cm ⁻¹)	Assignment
2080	SiH ₂ stretch
2000	SiH stretch
890	SiH ₂ bend-scissors
630	SiH bend:SiH ₂ rock
1015	SiF ₄ stretch
930	SiF ₂ stretch
830	SiF stretch
970 ^a	(SiF ₂) _n stretch
880 ^a	(SiF ₂) _n stretch

^aThese peaks appear with H₂ dilution, as in Fig. 8.

rock at 630 cm⁻¹.²⁶ A striking feature in these spectra is the shift of hydrogen from the SiH to the SiH₂ configuration with an increase in the fluorine content. Because the presence of SiH₂ is often associated with a decrease in film quality,²⁷⁻³⁰ we thoroughly investigated the conditions of its formation.

We first verified that the peak at 2080 cm⁻¹ is due to SiH₂ since the two are not necessarily equivalent.³¹ This absorption could also be caused by SiHF or by SiH in a blue-shifting environment. Theoretical calculations^{32,33} suggest that in the species SiHF, the Si—H stretch would be shifted to 2100 cm⁻¹, the Si—F stretching frequency would appear near 800 cm⁻¹, and an H—Si—F bending mode would appear near 900 cm⁻¹. Thus, the peaks at 2080, 890, and 830 cm⁻¹ could be caused by the species SiHF, rather than by SiH₂ and SiF. To distinguish between these assignments, we deposited *a*-Si:D:F films and measured the ir spectra.³⁴ The peaks attributed to H motions (at 2080, 2000, 890, and 630 cm⁻¹) are red-shifted on deuteration and the peaks attributed to F motions (at 1015, 930, and 830 cm⁻¹) are unshifted. This eliminates the possibility of SiHF, since the peak at 830 cm⁻¹ would also have been red-shifted to some degree.

Calculations predict that absorption at 2100 cm⁻¹ can also be due to SiH in environments such as on a Si atom with a dangling bond,³⁵ with a strongly electronegative second-neighbor atom,³⁵ on an internal surface,³⁶ or in a clustered phase.³⁷ SiH and SiH₂ can be distinguished by the SiH₂ bending modes at 870–890 cm⁻¹ and 840–850 cm⁻¹.³⁸ However, the second bending peak is not necessarily present in films with SiH₂. For example, it has been shown that by He-ion bombardment of *a*-Si:H, the strength of the 850-cm⁻¹ peak depends on the local environment and can be reversibly changed without changing the strength of the 890- and 2100-cm⁻¹ peaks.³⁹ It has been demonstrated with an rf glow discharge that, depending on the substrate potential, films can be deposited with only an 890-cm⁻¹ mode (cathodic) or with modes at both 850 and 890 cm⁻¹ (anodic).⁴⁰ These were attributed to isolated SiH₂ and polymeric (SiH₂)_n, respectively. In the present spectra there are peaks at 890 cm⁻¹ but not at 840–850 cm⁻¹. Figure 4 shows that the intensity of the 890-cm⁻¹ peak is proportional to that of the 2080-cm⁻¹ peak. This identifies the 2080- and 890-cm⁻¹ peaks as primarily due to isolated SiH₂. The nonzero intercept indicates that a small portion of the peak at 2080 cm⁻¹ is in fact due to SiH in a blue-shifting environment. The ratio of 2:1 for the stretch to the bend is the same as that found by others for glow discharge²⁶ and sputtered²² *a*-Si:H films. Note, however, that the SiH₂ bend is at a slightly higher frequency (890 versus 880 cm⁻¹) and has a narrower linewidth than is commonly observed for this species.²⁶ This suggests that the mode is perturbed by the increased electronegativity of the matrix.

2. Microstructure quantification

SiH₂ can appear on grain boundaries of microcrystalline silicon and on internal surfaces of amorphous silicon. To distinguish between these, Raman spectra were measured. At 7 at. % F content the transverse optical (TO)

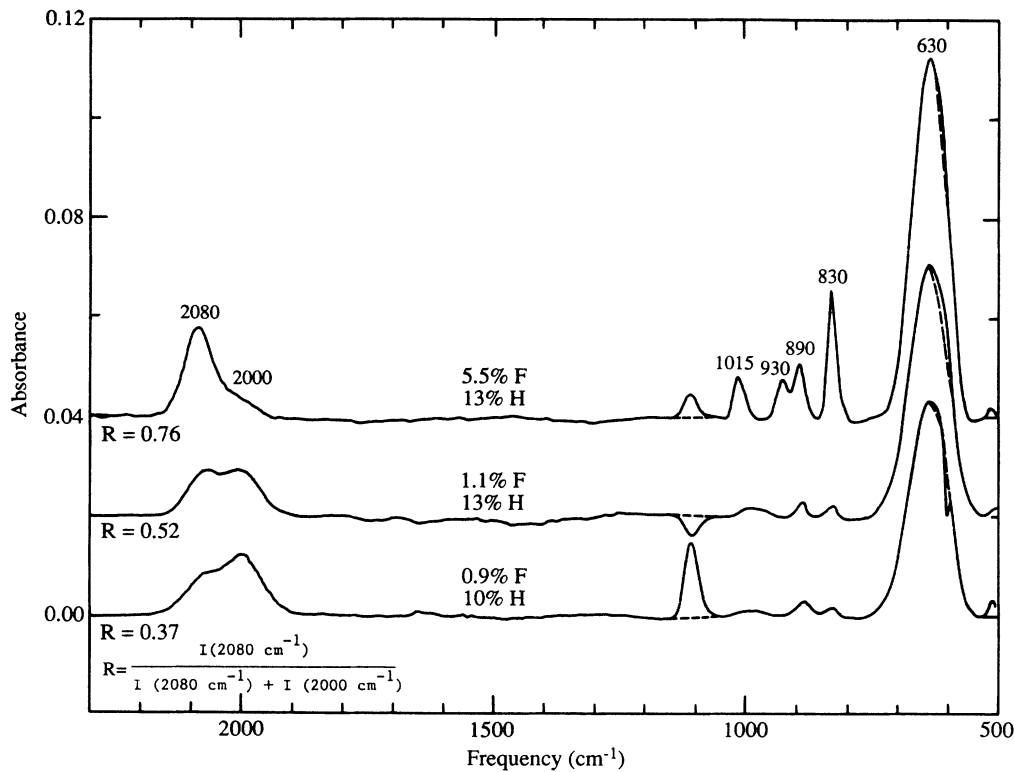


FIG. 2. Infrared spectra of *a*-Si:H:F films deposited at 245°C with a range of XeF₂ flow rates. For display, the spectra have been flattened by dividing by the baseline. The top film is 4200 Å thick and the other spectra have been normalized to this thickness. The spectra are vertically offset for clarity. Peaks attributed to silicon fluorides and hydrides are identified in Table II. Peaks at 1110 and 605 cm⁻¹ are due to the *c*-Si substrate.

phonon line is at 478 cm⁻¹ with a half-width on the high-frequency side of 32 ± 3 cm⁻¹. The peak position and linewidth are consistent with previous results for *a*-Si:F and *a*-Si:H:F.¹⁵ No sharp feature at 520 cm⁻¹

characteristic of a microcrystalline phase is present. Thus, the material is amorphous and the probable location of the SiH₂ is on internal surfaces rather than on grain boundaries.

To quantify this, the dihydride fraction, *R*, is defined²⁹ as the fraction of the integrated SiH_{*n*} stretching absorbance which is due to SiH₂:

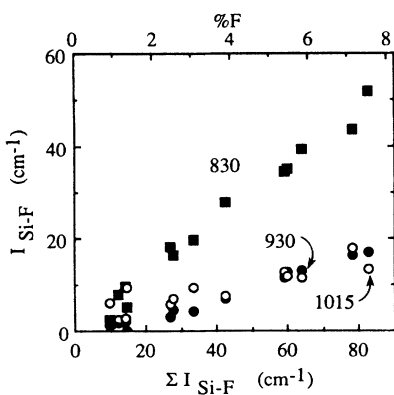


FIG. 3. Integrated strength of individual silicon fluoride peaks as a function of the total fluorine. The F content is represented by the sum of the integrated Si—F stretch absorbances and the calibration by XPS and EPMA is included on the top scale for reference. These films were deposited at 245°C with a range of XeF₂ flow rates.

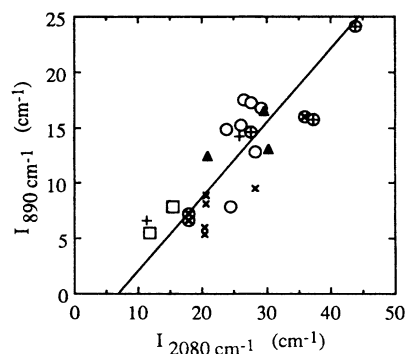


FIG. 4. Integrated absorption strengths of the SiH₂ stretch at 2080 cm⁻¹ and the bend at 890 cm⁻¹. The deposition conditions corresponding to each symbol are listed in Table I.

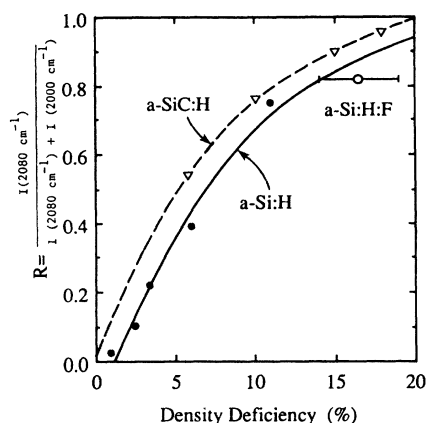


FIG. 5. Correlation between density deficiency and dihydride fraction R for a -Si:H and a -SiC:H from Ref. 41 and for an a -Si:H:F film from the present study.

$$R = \frac{I(2080 \text{ cm}^{-1})}{I(2080 \text{ cm}^{-1}) + I(2000 \text{ cm}^{-1})}$$

Since the oscillator strengths may differ for these species³⁷ and may be affected by fluorine incorporation,²² the fraction of the absorbance due to SiH_2 is not necessarily the fraction of hydrogen bonded as SiH_2 . Nevertheless, it is a useful parameter for the purpose of a comparison. A correlation between the parameter R and the density deficiency of glow discharge deposited a -Si:H and a -SiC:H has been established by Mahan *et al.*,⁴¹ who find that as R increases from 0 to 1 the density deficiency increases from 0 to 20%. This data is reproduced in Fig. 5. They attribute the density deficiency to film microstructure.

To confirm that the dihydride also indicates void formation in these films, the density of a fluorinated film was measured. A film with 6 at. % fluorine and $R = 0.82$ was found to have a density of $1.96 \pm 0.2 \text{ g/cm}^3$ measured by flotation in ZnBr_2 .⁴² The density deficiency is defined as the difference between the measured density and the density of crystalline Si containing fluorine. Upper and lower limits on the density of c -Si with 6 at. % F can be calculated by assuming either interstitial F (2.43 g/cm^3) or substitutional F (2.29 g/cm^3). Thus, the measured density corresponds to a 14–19% void fraction. Figure 5 shows that this fits the correlation of density deficiency with R found for a -Si:H.⁴¹ The nature of the film microstructure is not known simply on the basis of these results, but it is clear that these films contain voids in some configuration.

3. Correlation between F and SiH_2

The appearance of SiH_2 bonding with fluorine incorporation in the films is clearly demonstrated in Fig. 6(a). R tends toward zero, exclusively SiH bonding, with decreasing fluorine content and increases with increasing fluorine content. The variation of the fluorine content over the range of 1–7% almost completely changes the

configuration of the bonded hydrogen from SiH to SiH_2 . The increase in R is caused by a simultaneous increase in SiH_2 and decrease in SiH. Although exclusively SiH_2 bonding would give an R value of 1.0, in these films R appears to saturate at 0.8 for $T_S = 245^\circ\text{C}$ and at 0.5 for $T_S = 270^\circ\text{C}$.

For $T_S = 245^\circ\text{C}$, the correlation between F and R is the same whether the F content is changed by varying the XeF_2 flow or $P_{\text{Si}_2\text{H}_6}$. However, at $T_S = 270^\circ\text{C}$ the correlation between R and F in Fig. 6(a) is shifted down. The effect of substrate temperature is further demonstrated in Fig. 7. For fixed gas flow and composition, increasing the deposition temperature simultaneously decreases the film hydrogen content, fluorine content, and dihydride fraction R . With increasing T_S , note that the F content and R both reach minima at 300°C and do not change as the

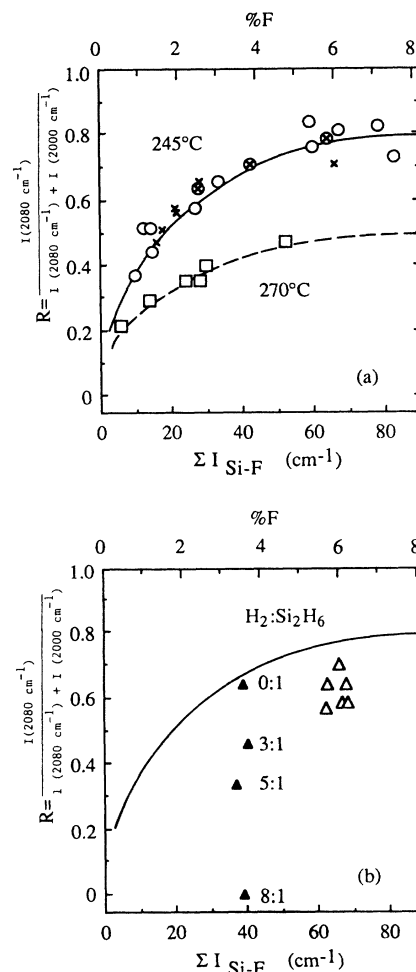


FIG. 6. Dihydride fraction R as a function of the F content for variations in (a) $P_{\text{Si}_2\text{H}_6}$ (\times), XeF_2 flow at 245°C (\circ), and XeF_2 flow at 270°C (\square), and (b) H_2 dilution with XeF_2 flow at 0.06 (\blacktriangle) and 0.12 (\triangle) sccm. The H_2 dilution ratios are identified for XeF_2 flow at 0.06 sccm. The same ratios were used as 0.12 sccm. The lines are drawn to guide the eye. The upper line from (a) is included in (b) for reference.

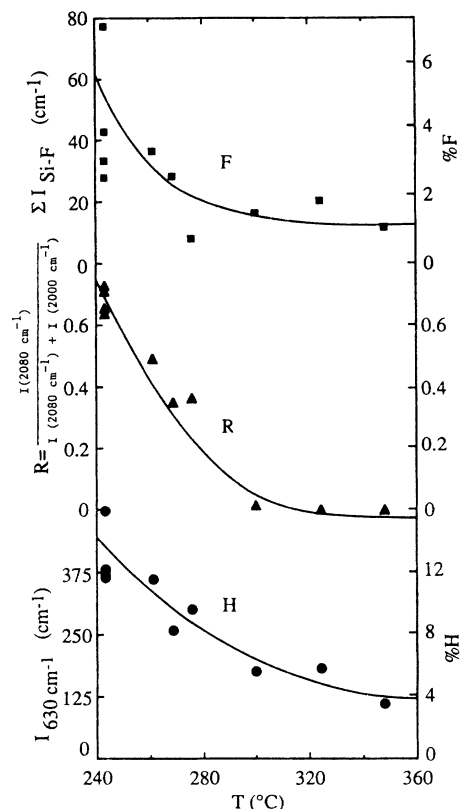


FIG. 7. Decrease in fluorine content R and hydrogen content with increasing substrate temperature. For reference, the integrated absorbances have been converted into percentages on the right axis. The lines are drawn to guide the eye.

temperature is increased further. In contrast, the H content decreases monotonically with T .

Dilution in H_2 with constant substrate temperature, XeF_2 flow, and Si_2H_6 flow produces a rather different correlation between F content and R [Fig. 6(b)]. Although the F content (and H content) are essentially unchanged, increasing dilution in H_2 decreases R . This is particularly striking with the lower XeF_2 flow rate where the dihydride is reduced below detection through H_2 dilution. Examining the spectra directly (Fig. 8) gives a more accurate picture of the effect of H_2 dilution. Although the total integrated absorbance of the fluorine peaks is unchanged with increasing H_2 dilution, the original Si—F peaks decrease in intensity and two broad peaks grow at 970 and 880 cm^{-1} . These broadened fluorine peaks look quite similar to those produced by high (approximately 36%) concentrations of F which we previously described and attributed to $(SiF_2)_n$.¹⁶ It appears that with hydrogen dilution, the material separates into a fluorine-rich phase with polymerized SiF_2 , and a phase with little fluorine in which the monohydride prevails.

B. Effect of F on optoelectronic properties

Optoelectronic properties are seriously degraded by the incorporation of fluorine. The $\eta\mu\tau$ product varies by 4 orders of magnitude over this range of deposition conditions. Although the scatter is large, the data show a trend of decreased $\eta\mu\tau$ with increased fluorine (Fig. 9). We have presented $\eta\mu\tau$ rather than the photoconductivity because the optical band gap increases from 1.75 to

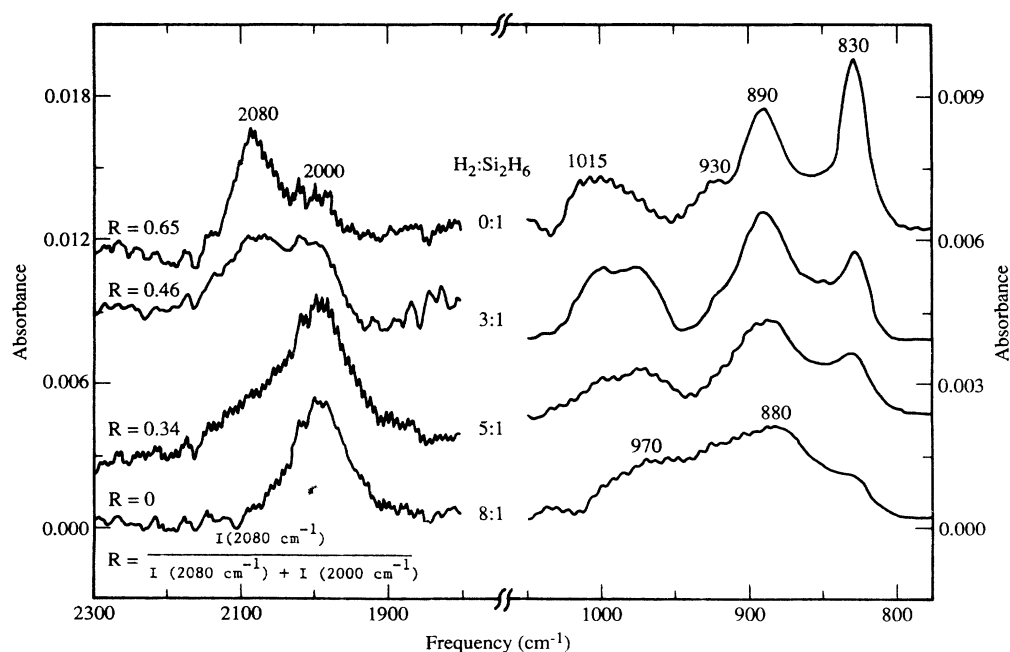


FIG. 8. Spectra of a -Si:H:F films deposited with XeF_2 flow at 0.06 sccm and varying $H_2:Si_2H_6$ ratios. All four films contain 3.6 at. % F and 12 at. % H. For display, the spectra have been flattened by dividing by the baseline. The bottom film is 1300 Å thick and the other spectra have been normalized to this thickness. The spectra are vertically offset for clarity.

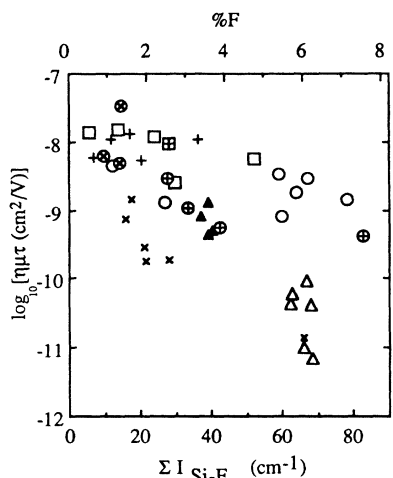


FIG. 9. Decrease in $\eta\mu\tau$ product with increase in fluorine content. The symbols are identified in Table I.

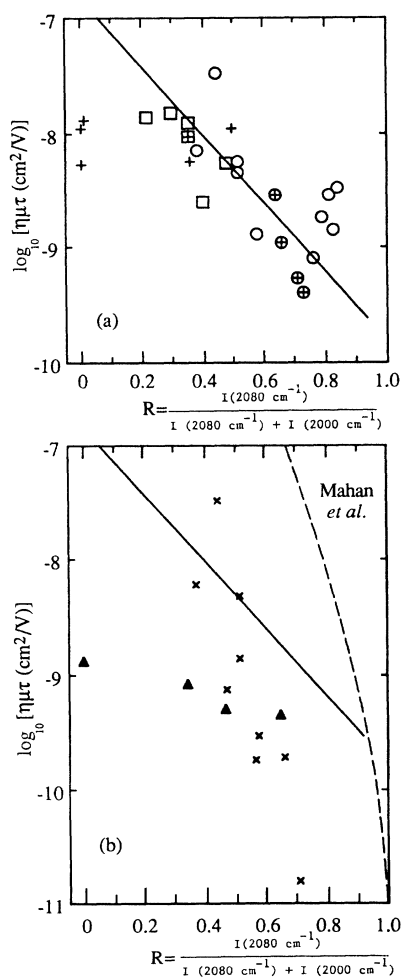


FIG. 10. Decrease in $\eta\mu\tau$ product with increase in dihydride fraction R for variations in (a) substrate temperature (+), XeF_2 flow at 245°C (O) and XeF_2 flow at 270°C (□), and (b) $P_{\text{Si}_2\text{H}_6}$ (×) and H_2 dilution with XeF_2 flow 0.06 sccm (▲). The line in (a) is drawn to guide the eye. In (b), the lines from (a) and from the $a\text{-Si:H}$ and $a\text{-SiC:H}$ data in Ref. 29 are included for comparison.

2.02 eV over this range of F and R .¹⁶ For all films measured, the dark conductivity activation energy is approximately half the band gap.

The decrease in $\eta\mu\tau$ also correlates with the increase in R . As either the XeF_2 flow or the substrate temperature is varied, the correlation between R and $\eta\mu\tau$ is the same [Fig. 10(a)]. It is interesting that the XeF_2 series and temperature series data fall on the same line, since the correlation between F and R changes with substrate temperature [Fig. 6(a)]. Three points from the temperature variation series do not seem to fit the correlation. For these points R is near zero but the $\eta\mu\tau$ product is lower than expected from the trend of the other data. These are the films deposited above 300°C where the F content and R no longer decrease with temperature but the H content does (see Fig. 7). Apparently in this regime the material continues to change with deposition temperature but R has reached zero and no longer describes material quality.

When either the disilane partial pressure or the hydrogen dilution is varied, rather different correlations between R and $\eta\mu\tau$ result [Fig. 10(b)]. The H_2 dilution series shows a smaller change with R and the $P_{\text{Si}_2\text{H}_6}$ series shows a greater change. For comparison, the correlation from Ref. 29 for $a\text{-Si:H}$ and $a\text{-SiC:H}$ is shown and it has a slope similar to the $P_{\text{Si}_2\text{H}_6}$ series. Thus, each series of films shows a correlation between R and $\eta\mu\tau$, but there is not a universal correlation.

IV. DISCUSSION

A. Comparison with previous studies

1. F content and SiH_2

Since the method of fluorine incorporation is unusual in these films, the general applicability of the results must be affirmed. An examination of the spectra in the literature indicates that in every $a\text{-Si:H:F}$ film with sufficient fluorine to see the SiF stretch at 830 cm^{-1} in the ir spectrum, SiH_2 also appears. This is true for films made from a variety of deposition techniques including sputtering of Si in Ar , SiF_4 and H_2 ,²³ dc or rf glow discharge of SiF_4 with H_2 or SiH_4 ,^{1,3,5,7,8,43,44} glow discharge of SiH_2F_2 ,⁴ reaction of H radicals with SiF_4 in a plasma,⁴⁵ and reaction of SiH_4 with F_2 .⁴⁵ In some of these reports spectra are shown at more than one fluorine level and the increase in R with the F content is evident.^{5,7,8,44,45} We showed an exception with H_2 dilution where the fluorine separates into a polymeric phase and the remaining hydrogenated phase does not exhibit dihydride bonding. Similar spectra were reported for films deposited by rf glow discharge of H_2 and SiF_4 .⁴⁶ However, when the H and F are not separated, the occurrence of the SiH_2 structure seems to be a universal result of fluorine incorporation.

Despite claims to the contrary, the films made by Matsumura *et al.*^{12,47,48} using either the reaction of SiF_2 and H or glow discharge deposition of SiF_2 and H_2 are not exceptions to this rule. This work must be mentioned

because the authors specifically claim to have deposited α -Si:H:F films which feature only monohydrides and fluorides. In the case of the first technique, the fluorine content was not measured, though the hydrogen content is reported to range from "a few" to "several" atomic percent. On the published ir spectra^{12,47} the dihydride is not evident, but neither is fluorine. The location of the expected SiF stretch is labeled but no peak is visible beyond the noise level. In the case of the second technique,⁴⁸ the peaks attributed to SiF and SiF₂ are located closer to 840 and 900 cm⁻¹ than the expected frequencies of 830 and 930 cm⁻¹. This suggests that they are actually the bending modes of (SiH₂)_n, which is consistent with the clear shoulder at 2100 cm⁻¹ on the SiH stretch peak. Thus, the spectra neither establish that these films actually do contain fluorine nor that they do not contain dihydrides, and so no exceptions have been found to the correlation between R and F .

2. DMR measurements

Nuclear magnetic resonance (NMR) can be used to probe deuterium (DMR) in deuterated amorphous silicon and provide structural information on the deuterium environment.^{49,50} In α -Si:D:H, the DMR line shapes, relaxation times, and temperature dependences are used to identify tightly bound D, weakly bound D located near the surfaces of microvoids, and molecular D₂ in the voids. A comparison of α -Si:D:F and α -Si:D:H films prepared by glow discharge of D₂ with SiF₄ or SiH₄, respectively, shows that the molecular deuterium line is significantly narrower in the fluorinated film.⁵¹ The decreased linewidth indicates an increased distance between the deuterium molecule and the void surface. The smallest void dimension is estimated to increase from 5.2 to 15 Å with fluorination. While the DMR study only reported on one α -Si:D:F film and it was necessarily deposited with hydrogen (deuterium) dilution, the primary finding agrees with the present results. The use of DMR for a systematic study of the effects of fluorine would be valuable.

B. Nature of microvoids

The dihydride fraction, R , is a rather indirect measure of microstructure. It is, however, more sensitive than either Raman spectroscopy, which did not distinguish between the highest F content films and nonfluorinated α -Si:H, or electron microscopy, which resolves features on the 100-Å scale. Density deficiencies as low as 2% can result in nonzero values of R (see Fig. 5). The exact nature of the voids which cause the density deficiency is unknown. They could be isolated microvoids or perhaps a network of low-density, hydrogen-rich regions analogous to grain boundaries in microcrystalline material.

The magnitude of the density deficiency is suggestive. In the film with 6 at. % F , the density deficiency is 14–19% and the H content is 13%. These are configured so that 6% of the Si is terminated with SiH or SiF, and 6% with SiH₂ or SiF₂. Thus, the ratio of missing Si atoms to dimer-terminated Si atoms to monoterminated

Si atoms is approximately 3:1:1. Moreover, the narrow ir linewidths suggest that the SiH and the SiF probably occur as isolated species in the lattice, thus reducing the ratio to 3:1. Since the appearance of SiH₂ and SiF₂ precludes the voids occurring exclusively as monovacancies, we must consider larger void sizes. Using the c - Si lattice for reference, a 2-atom vacancy has 6 Si atoms on the surface, a 3-atom vacancy has 8, and a 20-atom vacancy has a minimum of 26. Given the above 3:1 ratio, this indicates that the majority of the void surface is neither hydrogenated nor fluorinated. Since the spin density is several orders of magnitude too low for the voids to be lined with dangling bonds, the surface of the void must be predominantly tetrahedrally bonded Si which is reconstructed in a way analogous to the surface of crystalline silicon.

Since the ir spectra indicate that SiF₄ molecules are trapped in the films, it seems probable that they are located in the voids. For the film with 6 at. % F and a 14–19% density deficiency, approximately 0.3% of the Si occurs as SiF₄. If each void contains one SiF₄ molecule, the void size would be 50–60 atoms and the surface would contain 2 SiF₂ groups and 18 SiH₂ groups. This is consistent with the 40-atom void size measured by small-angle x-ray scattering (SAXS) in non-device-quality α -Si:H and in α -SiC:H.^{52,53}

The ir spectrum has features which support this model. The greater linewidths for SiF₂ and SiF₄ than for SiF (Figs. 2 and 8) could be caused by greater inhomogeneity in environment and is consistent with location in, or on the surface of, a void. The location of the SiH₂ bend at 890 cm⁻¹, blue-shifted from the typical value of 880 cm⁻¹, and the relatively narrow linewidth suggest an interaction of this mode with the electronegative fluorine in the matrix. If the SiH₂ lines a void which contains SiF₄, this provides a natural geometry for the interaction.

Further evidence for the location of SiF₄ in voids is the fact that it does not evolve from α -Si:H:F until the crystallization temperature of Si is reached.²³ It must, therefore, be in a site from which it cannot diffuse, which argues against an interstitial site. The picture of SiF₄ in voids is similar to the structural model of sputtered α -Si:F proposed by Matsumura *et al.*⁵⁴ From changes in the transmission electron microscopy (TEM) micrographs and ir spectra with anisotropic chemical etching, they found that the film consists of α - Si grains with SiF₄ and Ar at the grain boundaries.

The nature of the microstructure in the films changes when H₂ is introduced in the process gases. The ir spectra suggest that the material separates into a polymeric fluoride phase and a hydride phase. R tends toward zero with increasing H₂ dilution, indicating the disappearance of dihydride lined voids. However, the formation of (SiF₂)_n polymer chains probably creates a low-density network in the film. Thus, although R is not an appropriate description of the microstructure in these films, a heterogeneous structure is nonetheless indicated. A recent study shows that H₂ dilution of SiH₄ in the glow discharge deposition of α -Si:H also produces changes in the microstructure.⁵⁵ Gas-evolution measurements and

transmission electron microscopy suggest that H_2 dilution produces films with increased structural heterogeneity.⁵⁵

C. $\eta\mu\tau$ versus R correlation

The deterioration of electronic properties with the presence of dihydrides is well documented in the literature, though, of course, the absence of SiH_2 is not sufficient to guarantee high-quality material. For example, in a -Si:H formed by reactive sputtering, the dark and photoconductivity decrease as the dihydride density increases.²⁷ For a -Si:H deposited from silane and disilane plasmas, the ambipolar diffusion length decreases by an order of magnitude as the dihydride increases from 0 to 75 % of the bonded hydrogen.²⁸ For a -Si:H and a -SiC:H the $\eta\mu\tau$ product decreases by 3 orders of magnitude as the hydrogen bonding shifts from mono- to dihydride.²⁹ Polymeric dihydride chains have been associated with an increase in the rate of light-induced degradation.³⁰ Thus, the degradation in $\eta\mu\tau$ with increased dihydrides was not an unexpected result.

The results of Mahan *et al.*²⁹ show that the correlation between $\eta\mu\tau$ and dihydride fraction is the same for a -SiC:H and for a -Si:H deposited at elevated rf powers, but is quite different for a -SiGe:H. The data in Fig. 10(b) also show a decrease in $\eta\mu\tau$ with R , but again the exact behavior is different for each system. For the films deposited with H_2 dilution it is not surprising that $\eta\mu\tau$ depends only weakly on R because, as discussed above, the fluoride and hydride phases separate. Thus, $\eta\mu\tau$ does not increase as the dihydride decreases because the microstructure due to the $(SiF_2)_n$ polymer simultaneously increases. In the case of the data for varying $P_{Si_2H_6}$, an explanation for the results in Fig. 10(b) is not evident. The correlation between F and R for this data is identical to the data for XeF_2 flow variation at 245 °C [Fig. 6(a)], and yet the correlation between R and $\eta\mu\tau$ is different. Moreover, examination of the spectra shows that the Si—F peak widths and positions are similar for the two sets of films, suggesting similar microstructure. This indicates that neither the F content nor the dihydride content fully describes the film changes which are responsible for the degradation of the optoelectronic properties.

Recent experiments in our laboratory using SAXS suggest a reason for the lack of a unique correlation between the microvoid fraction and the photoconductivity.^{52,53} SAXS was used to obtain microvoid size, shape, and number density in a -Si:H deposited with different substrate temperatures and in a -SiC:H. In these films, there was a trend of decreased $\eta\mu\tau$ with increased void fraction, but, as in the present case, data for the different series of films did not lie on the same line. This appears to be caused by differences in the shape of the voids for different deposition series and differences in the gap-state densities.

D. Mechanism of void formation

There are several mechanisms by which fluorine incorporation could create dihydrides and microvoids. They

could be caused by fluorinated species trapped within the film, from the effect of fluorine on the chemistry of the growth surface, or from reactions of fluorinated species in the gas phase. These possibilities are considered below.

1. SiF_4 within voids

Some of the fluorine in the film is present as SiF_4 molecules, which could disrupt the silicon lattice sufficiently to force the formation of a void around them. As discussed above, the ir linewidths and positions of both the fluorides and hydrides, as well as annealing results, support the model of SiF_4 being located within the voids. The question here is whether the SiF_4 in the films actually causes the voids.

It is difficult to establish from our data that one particular fluoride species, such as SiF_4 , is responsible for the microstructure since, at a single substrate temperature, the fluorides occur at a fixed ratio to one another independent of total F concentration (Fig. 3). Thus, at each substrate temperature, equally good correlations between F content and R [as in Fig. 6(a)] can be drawn for each individual fluoride species and one cannot distinguish between causation and covariance. With increased substrate temperature, SiF_4 increases relative to SiF and SiF_2 from 20% of the total F content at 245 °C to 35% at 270 °C. If the void content were simply proportional to the concentration of SiF_4 , then for a given fluorine content R would be higher at the higher temperature. Figure 6(a) shows the opposite effect. This result does not rule out this mechanism since the substrate temperature can be expected to independently affect void formation (*vide infra*) as well as changing the ratio of the various fluoride species.

Data which support this model are found in films deposited with hydrogen dilution. The spectra in Fig. 8 show that with increasing H_2 dilution, the SiF_4 stretch and the SiH_2 stretch simultaneously decrease. The simple interpretation is that without SiF_4 to cause voids, there need be no dihydride to line voids. The actual case is more complicated. Since the formation of $(SiF_2)_n$ polymers may create voids of a different shape, with different surface structure, the lack of SiH_2 does not necessarily imply a lack of microstructure. In addition, H_2 dilution of the process gas can affect both the gas phase and surface reactions (discussed below), so it could be that the H_2 dilution reduces R through these channels, and that the disappearance of SiF_4 is coincidental.

2. Surface reactions

It has been demonstrated⁵⁶ that an increased sticking coefficient of the depositing species tends to produce defective material with increased microstructure. The sticking coefficient of silicon hydride fluoride radicals may be greater than that of radicals which do not contain fluorine. In addition, because of the greater strength of the Si—F bond, F atoms are not expected to diffuse on the surface as H atoms do. Thus, increased sticking coefficients or reduced surface mobilities of physisorbed fluorine-containing compounds could produce the in-

creased microstructure. The experimental parameter which affects the sticking coefficient and surface mobility is the substrate temperature. At increased T_S , the films have lower values of R for the same F content (Fig. 6), which supports the model that it is not fluorine incorporation in the film but rather the surface mobility of fluorinated species which affects the microstructure.

A parameter which, like the substrate temperature, increases the effective surface mobility is the introduction of H_2 in the process gases. Hydrogen gas is not directly photolyzed by 185-nm photons but hydrogen radicals are produced by the reaction



Hydrogen atoms are sufficiently unreactive with silanes to diffuse to the substrate surface, where they can etch Si—Si, Si—H, and Si—F bonds. Etching of weak bonds on the growth surface is similar to increasing the surface mobility of deposition species: both push the balance towards the thermodynamically favored species rather than the kinetically favored products. As in the case of increased substrate temperature, H_2 dilution of the process gas leads to increased clustering of the fluorine [as SiF_4 in the former case and $(SiF_2)_n$ in the latter] and decreased dihydride bonding. This serves as additional evidence that the large sticking coefficient of fluorides contributes to the increased microstructure of a -Si:H:F.

3. Gas phase reaction

A third possibility is that the gas phase reactions of fluorinated silanes favor precursors which produce dihydrides in the films. The high stability^{57,58} of the gas phase diradical $SiF_2(g)$ compared to $SiH_2(g)$ suggests some mechanisms for this. Whereas $SiH_2(g)$ readily inserts⁵⁹ into SiH_4 , thus reducing the direct contribution of diradicals to film growth,⁶⁰ $SiF_2(g)$ has a greater probability of reaching the growth surface intact. Since diradicals have higher sticking coefficients than monoradicals, this may lead to microstructure formation as discussed above. Another possibility is that fluorination of disilane increases the quantum yield of diradical decomposition products (i.e., SiF_xH_{2-x} and $Si_2F_yH_{4-y}$) over monoradicals. These diradicals could then either contribute to film growth directly, as discussed above, or insert into SiH_4 or Si_2H_6 to make higher-order silane polymers, which have also been shown to produce films with dihydrides.²⁸

In this deposition system there is evidence of such gas phase polymerization: powder was observed on the edge of the photolysis window.¹⁶ Since powder formation has not been previously observed for direct photo-CVD of Si_2H_6 with a Hg lamp, and is unexpected given the deposition rate of $<0.5 \text{ \AA/s}$, it appears to be a fluorine related phenomenon. Of course, it does not establish that increased polymerization with fluorinated process gases is a general phenomenon rather than a specific reaction of XeF_2 with Si_2H_6 .

It has been previously shown that gas phase polymerization can be reduced by the addition of H_2 .^{28,61} Thus, in the present case, the decrease in R with H_2 dilution is further evidence that gas phase polymerization may be the

cause of the dihydrides in the film. The mechanism for the suppression of gas phase polymerization by H_2 dilution is uncertain. The simplest explanation is the insertion of diradicals into H_2 to form closed-shell molecules, thus removing them without creating higher-order silanes. However, the rate constant for the insertion of $SiH_2(g)$ into H_2 has been measured to be 3 orders of magnitude smaller than for insertion into Si_2H_6 at 300 K.⁵⁹ Thus, ratios of $H_2:Si_2H_6$ on the order of 10^3 are required for removal of $SiH_2(g)$ by H_2 to become significant compared to the removal by Si_2H_6 . The maximum in these experiments is 8:1. Moreover, reaction of $SiF_2(g)$ with H_2 is undetectable.⁵⁸ Although a more complex mechanism must be invoked, it may indeed be through the reduction of gas phase polymerization that H_2 dilution reduces R .

Thus, there are three mechanisms through which fluorine could induce microvoids and all are consistent with the experimental results: SiF_4 in the film disrupting the lattice, reduced surface mobility of fluorinated species changing the growth surface, and changes in gas phase precursors. It is likely that all three contribute to the appearance of microstructure.

E. Contrast with crystallization and Si-Ge alloys

There are two other systems in which the use of fluorinated process gases has been shown to affect the film microstructure, μc -Si:H(F) and a -Si-Ge:H(F). In both cases the F content in the films, typically $<1\%$, is lower than in the present study. Nonetheless, our understanding of the role of F in the deposition can be expanded by considering these systems as well.

1. Crystallization

The increase in void content with F incorporation must be reconciled with the results showing that fluorinated process gases promote the growth of microcrystalline films.^{62–65} It appears that in one case the F disrupts the Si lattice and in the other it enhances the propagation of the Si network. In the latter case fluorinated process gases are employed but fluorine is not substantially incorporated in the films. Since, in both cases, fluorine should have the same effect on the gas phase reactions and the surface chemistry of the attachment of the precursors, it must be in the elimination of fluorine from the surface that they differ.

This gives support to those models of fluorine-enhanced crystallization which focus on the elimination of fluorine. For example, the importance of removing the H from grain boundaries to enhance the coalescence of the nuclei into larger crystallites has been recognized⁶⁶ and the release of HF in addition to H_2 has been proposed to enhance this.^{63,64} Hanna *et al.*⁶⁵ present an interesting refinement on the model of HF evolution wherein the Si—Si bond angle may inherit some regulation when HF is eliminated. In other words, the hydrogen bond between adjacent Si-H and Si-F will keep the silicons aligned along a bonding axis during growth. By contrast, adjacent Si-H and Si-H would tend toward a

staggered configuration due to steric hindrance. Thus, the evolution of HF with the formation of a Si—Si bond is more probable than the evolution of H₂, and it would also leave less lattice strain.

2. Si-Ge alloys

The present results must also be reconciled with work by Mackenzie *et al.*⁶⁷ on *a*-Si-Ge:H:F. They report an order of magnitude increase in the photoconductivity of alloys with band gaps near 1.5 eV deposited from (SiF₄ + GeF₄ + H₂) compared to (SiH₄ + GeH₄), and attribute the *improvement* to fluorine-induced changes in the microstructure. They use transmission electron microscopy to examine the microstructure. In TEM images of *a*-SiGe:H without F they see a two-phase heterostructure of dense "islands" of 100–200-Å diameter surrounded by lower-density "tissue" material. In the material deposited from fluorinated process gases the contrast in density between the phases increases and the boundaries become more angular.

These alloy films were deposited at a high enough substrate temperature (300 °C) that the F content of the films is < 1% as measured by electron microprobe, and dihydride bonding is not evident in the ir spectra. Because of the low F content, the changes are attributed not to the actual presence of F in the film but to the effect of F on the deposition process. Thus, the role of fluorine in this alloy deposition may not be comparable to that of the present study and is more akin to the microcrystallization process discussed above. Furthermore, although electron diffraction indicates that these films remain amorphous, the nature of the changes in the TEM (more density contrast and greater angularity in the islands) suggests that fluorinated process gases are pushing these films in the direction of microcrystallinity. Evidence that these films may be approaching the amorphous to microcrystalline transition comes from Nakano *et al.*⁶⁸ who found by Raman spectroscopy that *a*-SiGe:H:F deposited with the same process gases is partially crystallized when $T_S > 220$ °C, although this comparison is limited because the deposition pressure, flow rates, and power are all critical parameters.

Interestingly, the ir spectra of Si—F stretches in *a*-SiGe:H:F (Ref. 67, Fig. 13) look similar to those in Fig. 8 for *a*-Si:H:F deposited with H₂ dilution. Both have a broad background absorption with two maxima in the 800–1000-cm⁻¹ range and with a small SiF band near 830 cm⁻¹ superimposed on the broad absorption. We have interpreted these broad peaks as an indication that the F is polymerized in a separate phase rather than uniformly dispersed. This is consistent with the TEM picture of two phases and suggests that the tissue region is fluorine rich. This is also consistent with the thermodynamic argument that, because of the chemical equilibrium between the SiF_{*n*} species, they must exist as a separate phase in *a*-SiGe:H:F.⁶⁹ The similarity of the *a*-SiGe:H:F spectrum to that of *a*-Si:H:F deposited with H₂ dilution may indicate that there are two factors contributing to the differences in these silicon germanium alloys with and without fluorine: the fluorination of the process

gases and the dilution in H₂. Interestingly, both these factors can be used to induce crystallization and so both are consistent with the changes in the TEM images. The researchers at Harvard are pursuing the investigation of the effect of H₂ dilution on structural and photoelectric properties of *a*-Si:H.⁵⁵

V. CONCLUSIONS

Increasing the fluorine content of *a*-Si:H:F films in the range of 1–7 % produces a shift in the hydrogen bonding configuration from SiH to SiH₂, as characterized by the dihydride fraction *R*. The dihydride has been previously correlated with microvoid formation and a density measurement confirms this for *a*-Si:H:F. This provides a conceptual model of a heterogeneous material: the matrix is amorphous silicon containing isolated SiH and SiF species, and within this matrix are voids which contain trapped SiF₄ molecules. The void surfaces are largely reconstructed Si but also contain SiF₂ and SiH₂. As the appearance of SiH₂ is a feature of every deposition technique reported in the literature which incorporates sufficient fluorine in the films to see the SiF stretch at 830 cm⁻¹, these results have wide application.

We found that the $\eta\mu\tau$ product decreases as the F content and *R* increase. This is in agreement with previous studies of *a*-Si:H and its alloys in which the dihydride has been associated with reduced film quality. The exact dependence of optoelectronic properties on dihydride formation is not universal; variations in different deposition parameters produce different correlations between $\eta\mu\tau$ and *R*. Nonetheless, in every series of films deposited there is a decrease in $\eta\mu\tau$ with increasing *R*. It appears that the hoped-for advantages of the strength of the Si—F bond are not realized because of the microstructural changes induced by fluorine. Therefore, we suggest that amorphous silicon with > 1% fluorine does not appear to be the material of choice of the intrinsic layer of photovoltaic devices.

Mechanisms by which fluorine can induce microstructure formation were considered. Three models are consistent with the data: SiF₄ forcing the creation of a void, defective lattice structure due to reduced surface mobility of physisorbed fluorinated species, and an increased number of diradicals either participating in film growth directly or causing gas phase polymerization.

Although fluorine incorporation is detrimental to *a*-Si:H:F, it may still prove to be useful for alloys with carbon or germanium where it has been reported to improve film properties.^{70–72} Fluorinated process gases used in conditions that give minimal fluorine incorporation in the films may also have advantages in the deposition of alloys^{67,68,73–75} and microcrystalline films.^{62–65} The latter two cases were contrasted with the present work and it appears that the benefit comes not from the actual presence of F in the film but from the process of its elimination from the growth surface.

ACKNOWLEDGMENTS

We are pleased to acknowledge the contributions of S. E. Asher in SIMS analysis, A. Nelson in XPS measurements, J. P. Goral and A. Mason in EPMA, J. Carapella in measuring the film density, and A. Mascarenhas in Ra-

man spectroscopy. Discussions with W. Paul, J. M. Jasinski, G. Lucovsky, R. Crandall, and H. Branz were particularly useful. This work was supported by the U.S. Department of Energy under contract No. DE-AC02-83CH10093.

- ¹A. Madan, S. R. Ovshinsky, and E. Benn, *Philos. Mag.* B **40**, 259 (1979).
- ²C. H. Hyun, M. S. Shur, and A. Madan, *Appl. Phys. Lett.* **41**, 178 (1982).
- ³Y. Kuwano, M. Ohnishi, H. Nishiwaki, S. Tsuda, and H. Shibuya, *Jpn. J. Appl. Phys.* **20**, Suppl. **20-2**, 157 (1981).
- ⁴U. C. Pernisz, L. Tarhay, J. J. D'Errico, and K. G. Sharp, in *Conference Record of the 19th IEEE Photovoltaic Specialists Conference* (IEEE, New York, 1987), p. 582.
- ⁵S. Usui, A. Sawada, and M. Kikuchi, *J. Non-Cryst. Solids* **41**, 151 (1980).
- ⁶D. E. Carlson and R. W. Smith, in *Conference Record of the 15th IEEE Photovoltaic Specialists Conference* (IEEE, New York, 1981), p. 694.
- ⁷Y. Uchida, T. Ichimura, O. Nabeta, Y. Takeda, and H. Haruki, *Jpn. J. Appl. Phys.* **21**, Suppl. **21-2**, 193 (1982).
- ⁸K. Nishihata, K. Komori, M. Konagai, and K. Takahashi, *Jpn. J. Appl. Phys.* **20**, Suppl. **20-2**, 151 (1981).
- ⁹H. Matsumura, Y. Nakagome, and S. Furukawa, *Appl. Phys. Lett.* **36**, 439 (1980).
- ¹⁰M. Janai, R. Weil, and B. Pratt, *Phys. Rev. B* **31**, 5311 (1985).
- ¹¹M. Janai, R. Weil, and B. Pratt, *J. Non-Cryst. Solids* **59&60**, 743 (1983).
- ¹²H. Matsumura, H. Ihara, H. Tachibana, and H. Tanaka, *J. Non-Cryst. Solids* **77&78**, 793 (1985).
- ¹³M. Kumeda, Y. Takahashi, and T. Shimizu, *Phys. Rev. B* **36**, 2713 (1987).
- ¹⁴S. R. Ovshinsky and D. Adler, in *Materials Issues in Applications of Amorphous Silicon Technology*, Vol. 49 of *Materials Research Society Symposium Proceedings*, edited by D. Adler, A. Madan, and M. J. Thompson (MRS, Pittsburgh, 1985), p. 251.
- ¹⁵R. Weil, I. Abdulhalim, R. Beserman, M. Janai, and B. Pratt, *J. Non-Cryst. Solids* **77&78**, 261 (1985).
- ¹⁶A. A. Langford, J. Bender, M. L. Fleet, and B. L. Stafford, *J. Vac. Sci. Technol. B* **7**, 437 (1989).
- ¹⁷A. A. Langford, B. L. Stafford, and Y. S. Tsuo, in *Conference Record of the 19th IEEE Photovoltaic Specialists Conference* (IEEE, New York, 1987), p. 573.
- ¹⁸S. Tsuo and A. A. Langford, U. S. Patent No. 4 816 294 (28 March 1989).
- ¹⁹J. Tauc, R. Grigorovici, and A. Vancu, *Phys. Status Solidi* **15**, 627 (1966).
- ²⁰M. H. Brodsky, M. Cardona, and J. J. Cuomo, *Phys. Rev. B* **16**, 3556 (1977).
- ²¹A. A. Langford, M. L. Fleet, and A. H. Mahan, *Sol. Cells* **27**, 373 (1989).
- ²²H. Shanks, C. J. Fang, L. Ley, M. Cardona, F. J. Demond, and S. Kalbitzer, *Phys. Status Solidi B* **100**, 43 (1980).
- ²³C. J. Fang, L. Ley, H. R. Shanks, K. J. Gruntz, and M. Cardona, *Phys. Rev. B* **22**, 6140 (1980).
- ²⁴M. Janai, L. Frey, R. Weil, and B. Pratt, *Solid State Commun.* **48**, 521 (1983).
- ²⁵A. A. Langford, M. L. Fleet, A. J. Nelson, S. E. Asher, J. P. Goral, and A. Mason, *J. Appl. Phys.* **65**, 5154 (1989).
- ²⁶G. Lucovsky, R. J. Nemanich, and J. C. Knights, *Phys. Rev. B* **19**, 2064 (1979).
- ²⁷F. R. Jeffrey, H. R. Shanks, and G. C. Danielson, *J. Appl. Phys.* **50**, 7034 (1979).
- ²⁸R. C. Ross and J. Jaklik, Jr., *J. Appl. Phys.* **55**, 3785 (1984).
- ²⁹A. H. Mahan, P. Raboisson, and R. Tsu, *Appl. Phys. Lett.* **50**, 335 (1987).
- ³⁰C. M. Fortmann, J. O'Dowd, and J. Newton, in *Stability of Amorphous Silicon Alloy Materials and Devices*, Proceedings of an International Conference on Stability of Amorphous Silicon Alloy Materials and Devices, AIP Conf. Proc. **157**, edited by B. L. Stafford and E. Sabisky (AIP, New York, 1987).
- ³¹W. Paul, *Solid State Commun.* **34**, 283 (1980).
- ³²W. B. Pollard and G. Lucovsky, *J. Phys. (Paris) Colloq.* **42**, C4-353 (1981).
- ³³W. B. Pollard and J. D. Joannopoulos, *Phys. Rev. B* **23**, 5263 (1981).
- ³⁴A. A. Langford, B. P. Nelson, M. L. Fleet, and R. S. Crandall (unpublished).
- ³⁵G. Lucovsky, *Solid State Commun.* **29**, 571 (1979).
- ³⁶H. Wagner and W. Beyer, *Solid State Commun.* **48**, 585 (1983).
- ³⁷H. R. Shanks, F. R. Jeffrey, and M. E. Lowry, *J. Phys. (Paris) Colloq.* **42**, C4-773 (1981).
- ³⁸M. Cardona, *Phys. Status Solidi B* **118**, 463 (1983).
- ³⁹S. Oguz, D. A. Anderson, W. Paul, and H. J. Stein, *Phys. Rev. B* **22**, 880 (1980).
- ⁴⁰C. C. Tsai and H. Fritzsche, *Sol. Energy Mater.* **1**, 29 (1979).
- ⁴¹A. H. Mahan, A. Mascarenhas, D. L. Williamson, and R. S. Crandall, in *Amorphous Silicon Technology*, Vol. 118 of *Materials Research Society Symposium Proceedings*, edited by A. Madan, M. J. Thompson, P. C. Taylor, P. G. LeComber, and Y. Hamakawa (MRS, Pittsburgh, 1988), p. 641.
- ⁴²P. Menna, A. H. Mahan, and R. Tsu, in *Conference Record of the 19th IEEE Photovoltaic Specialists Conference* (IEEE, New York, 1987), p. 832.
- ⁴³M. Konagai and K. Takahashi, *Appl. Phys. Lett.* **36**, 599 (1980).
- ⁴⁴Y. Nakayama, K. Akiyama, and T. Kawamura, *Jpn. J. Appl. Phys. Pt. 2* **22**, L754 (1983).
- ⁴⁵J. Hanna, S. Oda, H. Shibata, H. Shirai, A. Miyauchi, A. Tanabe, K. Fukuda, T. Ohtoshi, O. Tokuhiko, H. Nguyen, and I. Shimizu, in *Materials Issues in Amorphous-Semiconductor Technology*, Vol. 70 of *Materials Research Society Symposium Proceedings*, edited by D. Adler, Y. Hamakawa, and A. Madan (MRS, Pittsburgh, 1986), p. 11.
- ⁴⁶G. Ganguly, S. C. De, S. Ray, and A. K. Barua, *Sol. Energy Mater.* **17**, 237 (1988).
- ⁴⁷H. Matsumura and H. Tachibana, *Appl. Phys. Lett.* **47**, 833 (1985).
- ⁴⁸H. Matsumura and S. Furukawa, *J. Non-Cryst. Solids* **59&60**, 739 (1983).
- ⁴⁹D. J. Leopold, P. A. Fedders, R. E. Norberg, J. B. Boyce, and J. C. Knights, *Phys. Rev. B* **31**, 5642 (1985).
- ⁵⁰M. P. Voltz, P. A. Fedders, R. E. Norberg, W. Turner, and W. Paul, *J. Non-Cryst. Solids* **114**, 546 (1989).

- ⁵¹R. E. Norberg and P. A. Fedders, Solar Energy Research Institute Annual Subcontract Report No. SERI/STR-211-3352, 1988.
- ⁵²D. L. Williamson, A. H. Mahan, B. P. Nelson, and R. S. Crandall, *Appl. Phys. Lett.* **55**, 783 (1989).
- ⁵³A. H. Mahan, D. L. Williamson, and B. P. Nelson, in *Amorphous Silicon Technology—1989*, Vol. 149 of *Materials Research Society Symposium Proceedings*, edited by A. Madan, M. J. Thompson, P. C. Taylor, Y. Hamakawa, and P. G. LeComber (MRS, Pittsburgh, 1989), p. 539.
- ⁵⁴H. Matsumura, K. Sakai, Y. Kawakyu, and S. Furukawa, *J. Appl. Phys.* **52**, 5537 (1981).
- ⁵⁵S. M. Lee, S. J. Jones, Y. Li, W. A. Turner, and W. Paul, *Philos. Mag. B* **60**, 547 (1989).
- ⁵⁶C. C. Tsai, J. G. Shaw, B. Wacker, and J. C. Knights, in *Amorphous Silicon Semiconductors—Pure and Hydrogenated*, Vol. 95 of *Materials Research Society Symposium Proceedings*, edited by A. Madan, M. J. Thompson, D. Adler, and Y. Hamakawa (MRS, Pittsburgh, 1987), p. 219.
- ⁵⁷M. Janai, S. Aftergood, R. B. Weil, and B. Pratt, *J. Electrochem. Soc.* **128**, 2660 (1981).
- ⁵⁸A. C. Stanton, A. Freedman, J. Wormhoudt, and P. P. Gaspar, *Chem. Phys. Lett.* **122**, 190 (1985).
- ⁵⁹J. M. Jasinski and J. O. Chu, *J. Chem. Phys.* **88**, 1678 (1988).
- ⁶⁰A. Gallagher, *J. Appl. Phys.* **63**, 2408 (1988).
- ⁶¹J. W. Perry, Y. H. Shing, and C. E. Allevato, *Appl. Phys. Lett.* **52**, 2022 (1988).
- ⁶²A. Matsuda, S. Yamasaki, K. Nakagawa, H. Okushi, K. Tanaka, S. Iizima, M. Matsumura, and H. Yamamoto, *Jpn. J. Appl. Phys. Pt. 2* **19**, L305 (1980).
- ⁶³N. Shibata, K. Fukuda, H. Ohtoshi, J. Hanna, S. Oda, and I. Shimizu, in *Amorphous Silicon Semiconductors—Pure and Hydrogenated*, Vol. 95 of *Materials Research Society Symposium Proceedings*, edited by A. Madan, M. J. Thompson, D. Adler, and Y. Hamakawa (MRS, Pittsburgh, 1987), p. 225.
- ⁶⁴S. Nishida, T. Shiimoto, A. Yamada, S. Karasawa, M. Konagai, and K. Takahashi, *Appl. Phys. Lett.* **49**, 79 (1986).
- ⁶⁵J. Hanna, A. Kamo, M. Azuma, N. Shibata, H. Shirai, and I. Shimizu, in *Amorphous Silicon Technology*, Vol. 118 of *Materials Research Society Symposium Proceedings*, edited by A. Madan, M. J. Thompson, P. C. Taylor, P. G. LeComber, and Y. Hamakawa (MRS, Pittsburgh, 1988), p. 79.
- ⁶⁶A. Matsuda, *J. Non-Cryst. Solids* **59&60**, 767 (1983).
- ⁶⁷K. D. Mackenzie, J. H. Burnett, J. R. Eggert, Y. M. Li, and W. Paul, *Phys. Rev. B* **38**, 6120 (1988).
- ⁶⁸S. Nakano, Y. Kishi, M. Ohnishi, S. Tsuda, H. Shibuya, N. Nakamura, Y. Hishikawa, H. Tarui, T. Takahama, and Y. Kuwano, in *Materials Issues in Applications of Amorphous Silicon Technology*, Vol. 49 of *Materials Research Society Symposium Proceedings*, edited by D. Adler, A. Madan, and M. J. Thompson (MRS, Pittsburgh, 1985), p. 275.
- ⁶⁹Y. Okada, D. Slobodin, S. F. Chou, R. Schwarz, and S. Wagner, in *Materials Issues in Amorphous-Semiconductor Technology*, Vol. 70 of *Materials Research Society Symposium Proceedings*, edited by D. Adler, Y. Hamakawa, and A. Madan (MRS, Pittsburgh, 1986), p. 289.
- ⁷⁰T. Uesugi, H. Ihara, and H. Matsumura, *Jpn. J. Appl. Phys. Pt. 1* **24**, 1263 (1985).
- ⁷¹A. H. Mahan, D. L. Williamson, M. Ruth, and P. Raboisson, *J. Non-Cryst. Solids* **77&78**, 861 (1985).
- ⁷²S. Guha, *J. Non-Cryst. Solids* **77&78**, 1451 (1985).
- ⁷³S. Oda, S. Ishihara, N. Shibata, S. Takagi, H. Shirai, A. Miyauchi, and I. Shimizu, *J. Non-Cryst. Solids* **77&78**, 877 (1985).
- ⁷⁴S. Aljishi, D. S. Shen, V. Chu, Z. E. Smith, J. P. Conde, J. Kolodzey, D. Slobodin, and S. Wagner, in *Amorphous Silicon Semiconductors—Pure and Hydrogenated*, Vol. 95 of *Materials Research Society Symposium Proceedings*, edited by A. Madan, M. J. Thompson, D. Adler, and Y. Hamakawa (MRS, Pittsburgh, 1987), p. 323.
- ⁷⁵K. D. Mackenzie, J. Hanna, J. R. Eggert, Y. M. Li, Z. L. Sun, and W. Paul, *J. Non-Cryst. Solids* **77&78**, 881 (1985).